Measuring the Thicknesses of Auroral Curtains

JOSEPH E. BOROVSKY,[1] DAVID M. SUSZCYNSKY,[1] MELVIN I. BUCHWALD[2]
and HAROLD V. DeHAVEN[2]

ABSTRACT. Auroral arcs (curtains) are extremely thin. A calculation of the minimum-possible arc thickness is presented; this minimum thickness is found to be about 9.5 m. Four requirements for designing an optical system that can image the thinnest curtains are discussed: 1) angular resolution, 2) temporal resolution, 3) light-gathering power, and 4) data-recording convenience. An optical system meeting these four requirements was constructed. With this system, an observing campaign in Fort Smith, Northwest Territories, has begun and images of the small-scale structure of auroral arcs are presented. Arc thicknesses of approximately 40 m were observed. These measurements of arc thicknesses may provide a critical test for the many theories about the origins of auroral arcs.

Key words: aurora, geomagnetism, ionosphere, Northwest Territories, photography, polar

RÉSUMÉ. Les arcs auroraux (draperies) sont extrêmement minces. On présente un calcul de l'épaisseur minimale possible d'un arc, qui se révèle être de l'ordre de 9,5 m. On discute des quatre éléments nécessaires à la conception d'un système optique qui puisse imager les draperies les plus minces, soit: 1) la résolution angulaire, 2) la résolution temporelle, 3) la capacité de captage de la lumière et 4) la facilité de collecte des données. On a construit un système optique qui répond à ces quatre critères et avec lequel on a commencé une campagne d'observation à Fort Smith dans les Territoires du Nord-Ouest. On présente des images de la structure à petite échelle des arcs auroraux. On a observé des épaisseurs d'arcs d'environ 40 m. Ces mesures de l'épaisseur des arcs peuvent servir à vérifier les multiples théories concernant l'origine des arcs auroraux.

Mots clés: aurore boréale, géomagnétisme, ionosphère, Territoires du Nord-Ouest, photographie, polaire

Traduit pour le journal par Nésida Loyer.

AURORAL ARCS

Auroral arcs are thin curtains of glowing air caused by thin sheets of energetic electrons precipitating down the earth's magnetic field into the upper atmosphere in the polar regions. A photograph of such an arc appears in Figure 1 and an idealized cut-away view of an arc appears in Figure 2. The arcs are typically aligned in an east-west direction and an arc can extend thousands of kilometres in this direction. The bottom edges of arcs are 95-110 km in altitude and the tops of the arcs are not well defined. The curtains are aligned with the earth's magnetic field, so the curtains are nearly, but not exactly, vertical. Arcs often have undulations and tight curls, the latter appearing as bright vertical rays in the curtains. General reviews of arcs and other auroral phenomena can be found in the books by Eather (1980) and Akasofu (1979).

Auroral arcs are associated with sheets of intense electrical current (Wallis, 1976) that lie within a global electrical-current pattern extending from the outer reaches of the earth's magnetic field to the upper atmosphere. The currents in this global pattern flow along the earth's magnetic field lines and connect to the upper atmosphere in two large rings around the earth's magnetic poles. These rings are known as the auroral ovals, or the auroral zones, and it is in these two ovals that the auroral arcs and other auroral forms are found. The positions of the auroral ovals depend on the level of activity of the sun. During normal solar activity the southern auroral oval lies entirely over water and over Antarctica. In the Northern Hemisphere (Fig. 3) the auroral oval typically cuts across Fairbanks, Alaska; Fort Smith, Northwest Territories; Churchill, Manitoba; Port Harrison, Quebec; and Fort Chimo, Quebec. From there it passes south of Greenland, skirts the northern coast of Scandinavia, then grazes the northern coast of western Siberia before cutting back through central Alaska (Oliver *et al.*, 1960:Fig. 15-45; Lanzerotti and Uberoi, 1988:Fig. 3).

Auroral arcs are the final link in a chain of processes that transfer electrical energy from the sun to the earth. The sun gives off a tenuous wind of charged particles that blows past the earth at 400-500 km·sec^{-1}. This solar wind couples to the earth's magnetic field, driving the electrical current system that flows through the auroral zone (Axford and Hines, 1961; Sato and Iijima, 1979). A fraction of the energy transferred from the solar wind to the earth's magnetic field goes into energizing the electrons that produce the auroral arcs. The energization apparently takes place in very localized regions high above the earth and the electrons leave the localized regions in narrow sheets and travel downward along the geomagnetic field lines, where they subsequently deposit their energy into the upper atmosphere in the polar regions. How the energy is transferred to the electrons is still a mystery, although several theories have been put forth. The study of auroral arcs promises to provide information about the energy-coupling processes. Auroral arcs are also associated with the emission of radio waves that can be detected far from the earth (Benson and Akasofu, 1984) and auroral arcs are associated with the lifting of oxygen and hydrogen out of the upper atmosphere (Johnson, 1983). Hence, the study of auroral arcs promises to lead to better interpretations of signals detected in radio astronomy and to a better understanding of the transport of material from the earth into outer space. On a more practical level, auroral arcs produce radio noise and enhanced ionization columns in the upper atmosphere, both of which interfere with radio and television communication in the polar regions (Kirby, 1982). The study of auroral arcs may lead to a better understanding of this interference, if not to a predictive or preventive capability.

This paper concerns the motivation, design, and implementation of an imaging system that is used for measuring the thicknesses of auroral arcs. The current knowledge about auroral-arc thicknesses is overviewed, predictions of the minimum thickness that an auroral arc can have are presented,

[1]Space Plasma Physics Group, Los Alamos National Laboratory, Los Alamos, New Mexico 87545, U.S.A.
[2]Atmospheric Sciences Group, Los Alamos National Laboratory, Los Alamos, New Mexico 87545, U.S.A.

FIG. 1. Three auroral arcs photographed over Yellowknife, N.W.T. (photograph courtesy of David Forbes).

North - South Cross Section
of Auroral Arc (Curtain)
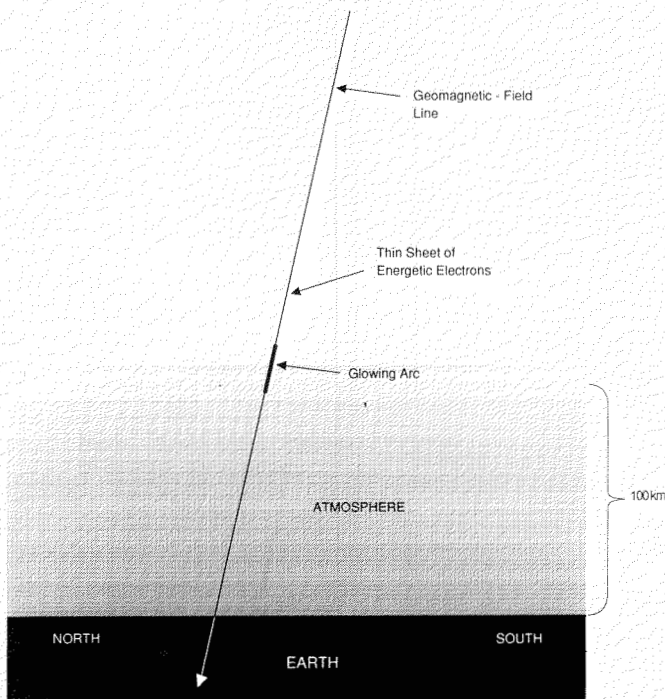
FIG. 2. A depiction of an auroral arc (curtain) in the upper atmosphere and the sheet of energetic electrons precipitating down to produce the glow.

a measuring system that was constructed and then fielded in Fort Smith, Northwest Territories, is described, and preliminary data obtained with that system are previewed.

CURRENT UNDERSTANDING ABOUT ARC THICKNESSES

Since auroral arcs are the glowing footprints of sheets of energetic electrons, measurements of the thicknesses of auroral arcs can be compared with predictions about the thicknesses of the electron-energization zones to provide direct tests of the competing theories for the origin of auroral

arcs. In the various theories, electrons are energized by electric fields associated with mechanisms named anomalous resistivity (Galeev, 1983), the thermoelectric effect (Hultqvist, 1971), the magnetic-mirror effect (Lennartsson, 1977), electrostatic shocks (Swift, 1979), double layers (Borovsky and Joyce, 1983), intermittent double layers (Lotko, 1986), Alfven waves (Haerendel, 1983), and plasma waves (Bingham *et al.*, 1988). In these theories, the electric fields are caused by processes called plasma flows (Rostoker and Bostrom, 1976), magnetic field reconnection (Goldstein and Schindler, 1978), wave coupling (Goertz, 1984), or ionospheric perturbations (Ogawa and Sato, 1971). (Another theory involving natural lasers [Calvert, 1987] does not involve electron energization.) Elaborating upon these theoretical models and working through the predictions of the thicknesses of auroral arcs is beyond the scope of this article; the various models predict thicknesses that range from a few hundred metres to several tens of kilometres.

One would think that satellites could be used to directly measure the thicknesses of auroral arcs, since there are a number of instrumented satellites that pass through the auroral zone. Indeed, satellite data do indicate the presence of small-scale structures in the auroral zone (e.g., Bankov *et al.*, 1986). However, two factors greatly limit the usefulness of satellites in directly measuring very small-scale auroral structures (Borovsky, 1988): 1) temporal variations cannot be distinguished from spatial variations and 2) the resolution of satellite instrumentation is insufficient. On the first point, each measurement a satellite makes is at a different point in space and at a different time; hence if a satellite instrument detects a sudden change, it cannot be determined whether that change was caused by the satellite crossing a boundary (spatial) or whether something turned on or turned off (temporal). On the second point, the faster satellite instruments typically take measurements a few times per second; since the satellites move at about 7 km·sec^{-1} this corresponds to measurements being taken every 1 km or so, which is insufficient to measure (or even detect) structures much smaller than 1 km. Rocket-launched instrumentation offers some improvement, with measurements sometimes taken every 150 m or so (e.g., McFadden *et al.*, 1990). However, this still does not resolve the smallest auroral structures and it still does not allow spatial variations to be discerned from temporal variations.

Likewise, satellite-based imaging systems are not of use in determining the thicknesses of auroral arcs. These imaging systems (Chubb and Hicks, 1970; Anger *et al.*, 1973; Rogers *et al.*, 1974; Hirao and Itoh, 1978; Frank *et al.*, 1981; Anger *et al.*, 1987) lack the angular resolution necessary to see subkilometre-sized auroral features. Under the best conditions, the highest-resolution imager can resolve a 3 km structure. Space-based imagers are much better suited to following the large-scale motions of auroral arcs (Murphree *et al.*, 1989) or to observing the global dynamics of the entire auroral oval (Frank *et al.*, 1985).

Ground-based auroral-imaging systems have been either all-sky cameras (Stoffregen, 1962), television cameras (Davis, 1966), CCD (charge-coupled device) cameras (Ono *et al.*, 1987), or scanning photometers (Sawchuk and Anger, 1972). Besides having been used for arc-thickness measurements, those systems have also been used to investigate the spatial distribution of arcs (Lassen and Danielsen, 1989), the kinking and curling up of arcs (Hallinan and Davis, 1970), the
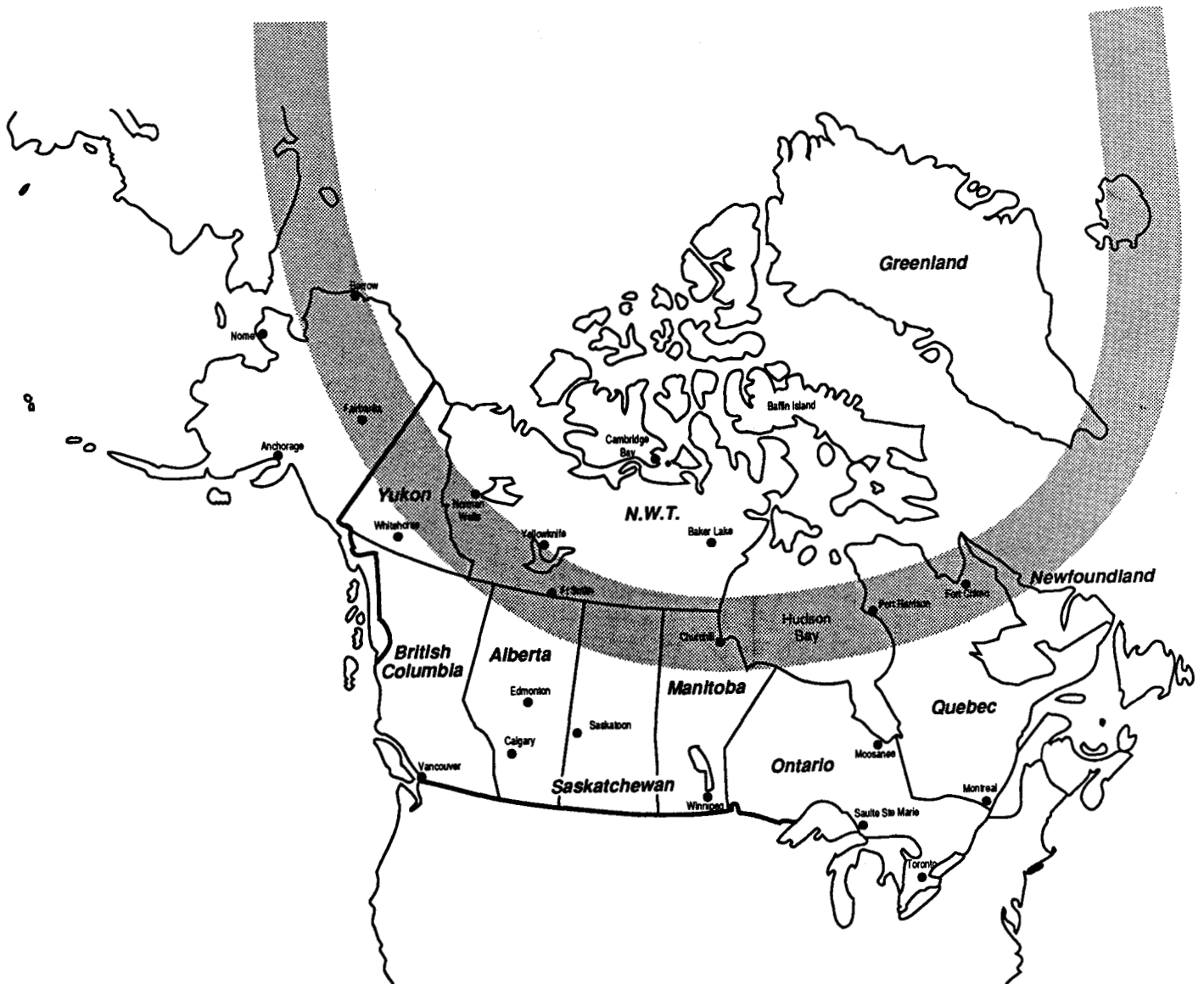
FIG. 3. The approximate position of the auroral oval (shaded region) during geomagnetically quiet times.

flickering of arcs (Beach *et al.*, 1968), the multiplicity of arcs (Davis, 1978), and the evolution of auroral-arc systems (Oguti *et al.*, 1988). The earliest recorded measurement of the thickness of an auroral arc is by Stormer (1955), who measured the thickness of a single auroral arc in September 1930 over Oslo, Norway, by photographing it in the magnetic zenith (looking up the geomagnetic field lines): a thickness of 7.4 km was obtained. Elvey (1957) used an all-sky camera at College, Alaska, to determine the thickness of one arc, obtaining a value of 250 m. Akasofu (1961) used a film camera with a wide-angle lens and a 1-second exposure in College, Alaska, to determine the thickness of one arc at two points, obtaining values of 336 m and 144 m. Kim and Volkman (1963) used an all-sky camera at Churchill, Manitoba, to measure the thicknesses of 40 arcs, obtaining values that ranged from 3.5 to 18.2 km. Maggs and Davis (1968) used an image-orthicon television system to measure the thicknesses of arcs in College, Alaska, over a five-day period. With 875/2 lines of video information on a 12° × 16° field of view, their resolution was 70 m for an object 100 km distant,

and they detected many 70 m thick arcs. From the trend in their histogram of the number of occurrences versus the arc thickness (Maggs and Davis, 1968:Fig. 2), it can be concluded that many arcs were not resolved by the imaging system. Indeed, the arc size that occurred most frequently on that histogram was the smallest size resolvable.

CALCULATION OF THE MINIMUM THICKNESS OF A CURTAIN

In designing an imaging system that will fully resolve auroral structures, a minimum scale size to be resolved must be decided upon. To obtain that minimum scale size, a theoretical calculation of the minimum possible thickness that an arc can have is performed. (The details of this calculation are deferred to the Appendix.)

The cause of the minimum thickness is the following. As electrons travel down the earth's magnetic field lines they suffer many random deflections as they hit the gas atoms of the upper atmosphere. These random deflections will spread the electrons out, so even if they form an infinitely

thin sheet high above the atmosphere, they will broaden into a sheet with a non-zero thickness in the upper atmosphere. The glowing arc will be at least as thick as this broadened sheet of electrons, no thinner. There is no point in designing an optical system to resolve smaller structures, since smaller auroral structures cannot exist.

To calculate the minimum thickness of arcs, the trajectories of energetic electrons are calculated with the aid of a computer (see Appendix) and the width of the region where the electrons transfer their energy to the air is determined. The electron trajectories are governed by three processes: 1) spiraling along the geomagnetic field lines, 2) slowing down owing to interaction with the atmospheric gas, and 3) scattering off the gas atoms.

To describe spiraling, the directed velocity of an electron is separated into components parallel and perpendicular to the magnetic field direction. The parallel component of the velocity is unaffected by the geomagnetic field, and so the electron moves along the geomagnetic field lines with a speed equal to this parallel velocity. The electron does not move across the magnetic field lines; rather, it travels around on a circle at a speed equal to the perpendicular component of the velocity. The radius of the circle depends on the magnitude of the perpendicular velocity and on the strength of the magnetic field. For auroral electrons in the upper atmosphere, the circles have radii that vary from 0 to about 10 m. The combination of the uninhibited motion along the magnetic field and the circular motion perpendicular to the field leads to a spiraling motion for the electrons (Fig. 4).

The slowing down of an electron as it enters the atmosphere is owed to collisions with gas atoms and molecules that result in energy transfer from the electron to the atoms and molecules. These collisions either excite or ionize the atoms and molecules. The de-excitation of an atom or molecule or its de-ionization usually results in the emission of one or more photons of light. It is exactly this light emission from the air atoms and molecules that is the glowing of the auroral curtain. Hence, keeping track of the amount of energy that the electrons lose (and where they lose it) determines more than just the rate of slowing down of the electrons: it determines how much light emission there will be from an arc and the shape of the glowing arc.

The scattering of an electron by a gas atom or molecule is the result of electrical forces on the electron when it passes through the atom or molecule and this deflects the electron's trajectory. Because of the deflection, the electron trajectory changes from one spiral to another (Fig. 4). The pitch and radius of the new spiral will differ from the pitch and radius of the old spiral. More important, the new spiral will be displaced from the old spiral. As it undergoes many scatterings, the electron suffers random displacements across the magnetic field lines. This will cause a group of electrons that all started out on the same geomagnetic field line to spread out onto other field lines. Hence, it is the scattering of electrons that broadens an arc and gives rise to the minimum thickness.

The results of the computer calculations are displayed in Figure 5. The trajectories of 1000 electrons of low energies and 1000 electrons of high energies that were in very thin sheets high above the atmosphere were followed. In the figure, the amount of energy lost to the atmosphere by the electrons is plotted versus the distance from the center of the sheet. The plot represents the intensity of the glow from the air

versus the distance from the arc center. Fitting the computer data with Gaussian curves, the full widths of the arcs are found to be 9.5 m for low-energy electrons and 24.6 m for
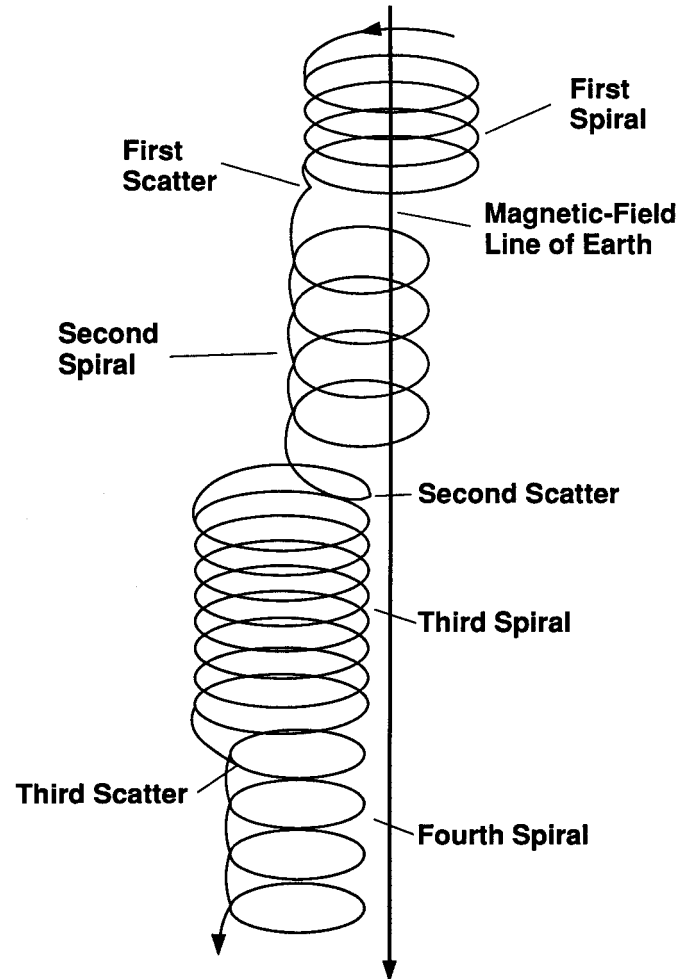
FIG. 4. A sketch depicting the displacement of an electron in the direction perpendicular to the magnetic field caused by collisions with gas atoms.
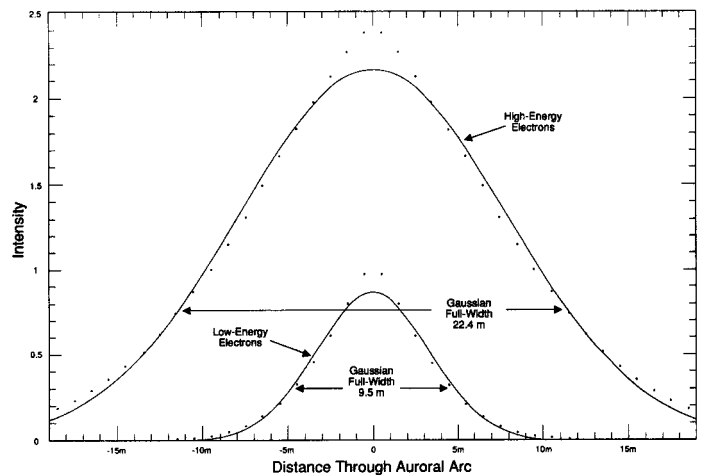
FIG. 5. Plots of the energy deposited by precipitating electrons as a function of the distance through an arc. The points are the computer data and the curves are Gaussian fits to the data. The electrons started out in an infinitely thin sheet; therefore, these are the profiles of the narrowest possible arcs. Details of the calculations from which these curves were generated appear in the appendix.

high-energy electrons. Accordingly, the minimum thickness of an auroral arc is predicted to be 9.5 m. The design criteria for imaging systems will be based upon this value.

REQUIREMENTS FOR THE IMAGING SYSTEM

Four requirements should be considered when designing an imaging system that will measure auroral-arc thicknesses by looking up the geomagnetic field lines (see Fig. 2). They are 1) angular resolution, 2) temporal resolution, 3) light-gathering power, and 4) data-recording convenience.

The first requirement has been alluded to throughout this paper: the imaging system should be capable of resolving auroral arcs with thicknesses of 9.5 m. With the bottom edges of arcs located about 105 km in altitude (Currie, 1955; Stormer, 1955), an angular resolution of 0.006° is required to resolve an arc 9.5 m thick. In fact, even higher resolution is desirable. If the light emission from the arc has a Gaussian profile with a full width of 9.5 m, then in order to satisfy the sampling theorem (International Telephone and Telegraph, 1968) so that the Gaussian will be properly resolved, the resolution points must be separated by no more than one-quarter of the full width of the Gaussian, which is a 2.4 m separation. This translates into a desired angular resolution of 0.0016°.

The second requirement is on the temporal resolution of the system. Because auroral arcs move, they must be imaged quickly to prevent blurring, which will make the arcs appear thicker than they actually are. Arcs can drift in the north-south direction with speeds of up to 1 km·sec^{-1} (Omholt, 1971), but typical velocities may be more like 100-200 m·sec^{-1} (Evans, 1959). At a speed of 200 m·sec^{-1}, arcs will move through a 9.5 m distance in 0.05 sec. Hence, shutter speeds or image-sampling times faster than or at least comparable to this time are desirable.

In addition to the blurring caused by overly long exposure times, there is a natural blurring of the curtains that arises from the slow de-excitation of gas atoms. After an air atom is excited by an auroral electron, it may take seconds for the atom to de-excite and emit a photon of light. During this time the sheet of electrons that produces the arc can move a considerable distance. The result is about 1 sec worth of blurring (afterglow) of the image of the electron sheet. It can be predicted that this afterglow region behind the moving arc is dimmer than the arc itself. If the image of the arc is not overexposed, then this afterglow region can be discerned from the arc. However, the proper exposure level for each arc cannot be predicted before the image is taken. Fortunately, this afterglow can be eliminated by using optical filters that pass only light of select wavelengths that correspond to very fast de-excitations of the air atoms. When an imaging system lets in all wavelengths (no selection), the image will be referred to as a "white-light" image, and when only selected wavelengths are let in, the image will be referred to as a "fast-filtered" image. Unfortunately, fast filtering removes light from the aurora, making the curtains dim.

This brings up the third requirement: light-gathering power. Short exposure times and fast filtering combine to greatly limit the amount of light available to form an image of an auroral arc. The light-gathering power of a system is improved by either using an imaging system with a lower f number (which means a larger aperture) or by using more sensitive image-recording methods (e.g., using faster film or electronic image intensifiers). The satisfaction of light-gathering requirements will be largely by trial and error, owing to the absence of information about the brightness of small-scale auroral structures.

The final requirement for the imaging system is a convenient method of data recording. Because of the time-resolution requirement cited above and because the structures will move rapidly through the field of view at unpredicted times, many images must be taken rapidly when an arc is near the magnetic zenith. Using photographic film as a recording medium will require the use of a movie camera on the back of the optical system. A drawback to this is that image-processing techniques that can eliminate noise on the images are difficult to implement when the images are recorded on photographic film. Electronically stored images are much easier to work with. Intensified television cameras connected to video-cassette recorders are ideal for the data collection and analysis, particularly because of the ease of image processing and because instantaneous viewing of the images is possible.

PRELIMINARY RESULTS OF ARC-THICKNESS MEASUREMENTS

Figure 6 is a diagram of the auroral-arc-imaging system that was used in April 1990 at the Environment Canada Upper-Air Station at Fort Smith, N.W.T. Of the readily accessible North American sites along the auroral oval (Fairbanks, Fort Smith, Churchill, Port Harrison, and Fort Chimo), Fort Smith has superior viewing in terms of annual number of cloudless days (Hare and Hay, 1974). This is particularly true for viewing the aurora in spring or fall.

The arc measurements were made with a 10-inch $f/6.3$ Schmidt-Cassegrain telescope (Meade model 2120-LX6) connected to a microchannel-plate-intensified television camera (Xybion model ISG-206) with manual gain control. The manual gain control makes it possible to determine the absolute brightness of the auroral structures. The focal length of the telescope is 1600 mm and the field of view of the telescope/camera system is 0.31° × 0.41°. This corresponds to a field of view of 560 m × 750 m at a distance of 105 km. The resolution is limited to 270 lines of video information, which yields a resolution of 2.1 m at a distance of 105 km.
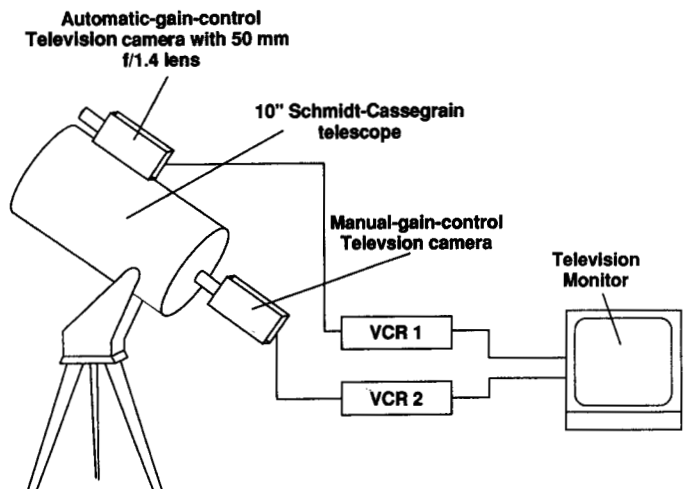
FIG. 6. The optical imaging system used in Fort Smith, N.W.T., to measure the thickness of auroral curtains.

This meets the desired resolution of 2.9 m set down in the last section. Unfortunately, when dim objects are imaged at the maximum gain setting of this Xybion camera, the resolution was observed to be five times worse than these values. Hence, for dim arcs, resolutions of about 10.5 m are obtained. Images are produced by the television camera thirty times per second, and each image is formed in 1/60 sec. Therefore, the temporal resolution is 1/60 sec = 0.017 sec, which exceeds the time-resolution requirement of the previous section. The telescope was run unfiltered to obtain white-light images and it was also run filtered to obtain fast-filtered images (using the 3914-Å emission from ionized nitrogen molecules). The telescope was pointed up the geomagnetic field lines, which at Fort Smith is 11°SSW of the zenith, and the arcs were seen edge on as they drifted through the field of view of the telescope.

Aligned with the telescope is a wider field-of-view television system used to determine when arcs are drifting into the field of view of the telescope (see Fig. 6). This "spotter" system is also used to correct the pointing of the telescope. The spotter system is composed of a microchannel-plate-intensified television camera (Xybion model ISS-01) with automatic gain control with a 50 mm f/1.4 lens attached. The automatic gain control simplifies the spotting of auroral structures with differing brightnesses. The field of view of the spotter system is 12° × 16°, which corresponds to 22 km × 29 km at a distance of 105 km. The image resolution is limited by a 242 × 377 array of pixels, which corresponds to a resolution of 91 m for objects that are 105 km away. When an arc passes through the field of view of the spotter system, the location of the magnetic zenith becomes obvious and the 10 inch telescope can be repointed to this location.

The video outputs of both television cameras are connected to separate VHS video-cassette recorders and then to a television monitor (see Fig. 6). The video-cassette recorders collected about five hours of data each night. The data was transported to Los Alamos, New Mexico, for analysis.

In the first segment of the observing campaign in Fort Smith, four full nights of auroral-arc imaging were obtained. Two of the nights were dedicated to white-light imaging and two to fast-filtered imaging. In the four nights that the imaging system was used, approximately 55 multiple-arc structures passed through the field of view of the spotter system. In the white-light images using the 10 inch telescope, each multiple arc contained 2-3 individual arcs. More may have been present, but image processing would be necessary to discern them. Because of the marginal light-gathering power, only one individual arc was seen with the 10 inch telescope during the two nights of fast-filtered data collection. A total of about 75 individual arc structures were imaged in white light with the 10 inch telescope.

Examples of the images obtained by the television cameras appear in Figures 7 and 8. A typical arc as seen by the spotter system appears in Figure 7. The field of view in the figure corresponds to 18 km × 24 km at the location of the arc. The arc is moving toward the bottom (south) at about 100 m·sec⁻¹. This arc consists of a broad envelope of diffuse emission with a width of about 8 km and a thinner band of emission inside. With the resolution of the spotter system, the thinner band of emission would appear to be about 600 m thick at its thinnest. When seen edge on by the 10 inch telescope, the thinner bands of emission are very thin and often consist of multiple bands.

FIG. 7. An auroral arc as seen by the spotter system looking up the earth's magnetic field lines. The field of view depicted is 10° × 13.4°. North is to the top and east is to the left.

A white-light auroral arc image as seen by the 10 inch telescope appears in Figure 8. The field of view in the figure is 515 m × 690 m. The arc is moving toward the bottom (south) at 220 m·sec⁻¹. The sky is darker ahead of the arc (at the bottom) than it is behind the arc (at the top). This is expected for the small spatial scale arcs, owing to the afterglow of the air atoms hit by the energetic electrons that produce the arc. The thickness of this arc as measured on the photograph is about 95 m. However, since the effective exposure time used to obtain this image was 0.13 sec (see the figure caption), the arc moved about 30 m during the exposure, and so it is probably about 30 m thinner than the 95 m value.

In previewing the data from the first campaign at Fort Smith, typical auroral arc thicknesses were found to be about 100 m, similar to that of Figure 8. The thinnest arc seen without image processing had a thickness of about 40 m. Hence, the suspicion that auroral arcs thinner than 70 m exist is confirmed.

In future campaigns, the auroral light will be selectively filtered by wavelength to improve the temporal resolution of the imaging system, television cameras with increased light sensitivity will be used to improve the light-gathering power, the f-number and focal length of the 10 inch telescope will be varied to improve the light-gathering power, and higher resolution video recorders will be used to improve the quality of the images. Additionally, the imaging system will be dedicated to the measurement of auroral arc thickness so that a much larger quantity of data will be obtained.

FIG. 8. An auroral arc as seen by the 10 inch telescope system looking up the earth's magnetic field lines. The field of view is 0.28° × 0.38°. The image was obtained from a multiple exposure of four consecutive video frames, each spaced by 1/30 sec. North is to the top and east is to the left.

ACKNOWLEDGEMENTS

APPENDIX: DETAILS OF THE THICKNESS CALCULATION

The computer program that follows the trajectories of the auroral electrons in the atmosphere does so by iterating among three operations: 1) solving the equations of motion for an electron in a uniform magnetic induction and advancing the position of the electron, 2) decreasing the velocity of the electron according to a Bethe stopping-power equation, and 3) determining a probability for elastic scattering off atmospheric gas atoms and scattering the electron.

The equations of motion for an electron in a uniform magnetic induction are (in cgs units)

$$\frac{\partial \vec{v}}{\partial t} = - \frac{e}{m_e c} \vec{v} \times \vec{B} \tag{1a}$$

$$\frac{\partial \vec{x}}{\partial t} = \vec{v} \tag{1b}$$

where $\vec{x}$ and $\vec{v}$ are the vector position and velocity of the electron, $\vec{B}$ is the magnetic induction, e and m_e are the electronic

charge and mass, and c is the velocity of light. The magnetic induction is taken to define the z-direction, and the x-direction is taken to be normal to $\vec{B}$ and to the sheet of electrons. Hence the arc will lie in the $y - z$ plane and the arc's width will be measured in the x-direction. The equations of motion (1a) and (1b) are computationally solved with a first-order time-centered numerical scheme.

Owing to the interaction of the electron with the atmospheric gas, the magnitude of its velocity $\vec{v}$ changes with time according to

$$\frac{\partial v}{\partial t} = \frac{\partial v}{\partial E} \frac{dE}{dx} \frac{\partial x}{\partial t} = \frac{1}{m_e} \frac{dE}{dx} \tag{2}$$

where dE/dx is the electronic stopping power of the atmospheric gas to an electron. The stopping power used is the Bethe formula for electrons (Eq. 4-124 of Marmier and Sheldon, 1969):

$$\frac{dE}{dx} = \frac{4\pi ne^4 Z}{m_e v^2} \left[\log \left(\frac{2v^2}{m_e I} \right) - 1.2329 \right] \tag{3}$$

where n is the number density of gas atoms, Z is the atomic number of the gas, I is the mean ionization potential of the gas, and log() is the natural logarithm. To estimate the number density n and atomic number Z as functions of the height h above the earth, the MSIS-86 atmospheric model (Hedin, 1987) is used for Fort Smith, N.W.T. (latitude 60.0°N, longitude 248.5°E) at midnight local time and during modest solar activity. The gas density data from the MSIS model is tabulated and linearly interpolated to the position of the electron for use in equation (3). The gas is dominantly nitrogen ($Z = 7$), the mean Z-value for 85-200 km altitudes being 7.2-7.3. The value $Z = 7.2$ was used in equation (3). The value of I is taken to be $I = 92$ eV, the suggested value of Ahlen (1980) for molecular nitrogen. Using expression (3) in equation (2), equation (2) is computationally solved with a first-order forward-difference numerical scheme.

The direction of $\vec{v}$ is changed according to a random probability and theoretical elastic-scattering cross-sections $\sigma(\theta,E)$ for fast-electron impact on nitrogen atoms. The values of the nitrogen cross-section data for 1-32 keV from Riley et al. (1975) and for 500 eV and 1500 eV from Fink and Ingram (1972) are used to produce a computational table of $\sigma(\theta,E)$ values, where θ is the angular deflection of the electron, E is the kinetic energy of the electron, and σ is the differential cross-section for scattering. Values of $\sigma(\theta)$ are tabulated every 1° for $0° \le \theta \le 10°$, every 10° for $10° < \theta \le 180°$, every 100 eV for $500 \text{ eV} \le E \le 2000$ eV, and every 1 keV for $2 \text{ keV} < E \le 32$ keV. The cross-sections for the nearest integer keV to the electron's kinetic energy are used. When discrete values of θ are considered, the probability of scattering through an angle of θ during a time Δt is

$$P(\theta) = \frac{1}{2\pi} \sigma(\theta) \Delta\theta \, v \, \Delta t \tag{4}$$

where $\Delta\theta$ is the separation of the discrete θ values. For the tabulations of the $\sigma(\theta)$ data, $\Delta\theta = 1°$ for $0° \le \theta \le 10°$ and $\Delta\theta = 10°$ for $10° < \theta \le 180°$. Whether or not a scattering occurs during a computational time step is determined by generating a random number R for each discrete θ value such that $0 \le R \le 1$; if $R \le P(\theta)$ then the scattering by θ occurs and if $R > P(\theta)$ then the scattering does not occur. The scattering is effected by generating a vector $\vec{u}$ of unit length and random direction normal to $\vec{v}$. The new value of $\vec{v}$ is given by

$$\vec{v}_{new} = \vec{v}_{old} \sin\theta + \vec{u} |\vec{v}_{old}| \cos\theta \tag{5}$$

The energy lost by each electron each time step

$$E_{lost} = \frac{dE}{dx} v \, \Delta t \tag{6}$$

is recorded as a function of x. This recording includes the energy lost by electrons that backscatter off the atmosphere. This energy lost will be directly proportional to the volume emission of light from the air. In Figure 5, low-energy electrons have 5 keV of kinetic energy and high-energy electrons have 25 keV.

Typically, about 130 seconds of cpu is required on a VAX 8700 computer to follow 1000 electrons with initial energies of 25 keV from $h = 200$ km to their terminations.

REFERENCES

AHLEN, S.P. 1980. Theoretical and experimental aspects of the energy loss of relativistic heavily ionizing particles. Reviews of Modern Physics 52:121-173.

AKASOFU, S.-I. 1961. Thickness of an active auroral curtain. Journal of Atmospheric and Terrestrial Physics 21:287-288.

———. 1979. Aurora Borealis. Alaska Geographic 6(2)1-95.

ANGER, C.D., BABEY, S.K., BROADFOOT, A.L., BROWN, R.G., COGGER, L.L., GATTINGER, R., HASLETT, J.W., KING, R.A., McEWEN, D.J., MURPHREE, J.S., RICHARDSON, E.H., SANDEL, W.R., SMITH, K., and VALLANCE JONES, A. 1987. An ultraviolet auroral imager for the Viking spacecraft. Geophysical Research Letters 14:387-390.

ANGER, C.D., FANCOTT, T., McNALLY, J., and KERR, H.S. 1973. ISIS-II scanning auroral photometer. Applied Optics 12:1753-1766.

AXFORD, W.I., and HINES, C.O. 1961. A unifying theory of high-latitude geophysical phenomena and geomagnetic storms. Canadian Journal of Physics 39:1433-1464.

BANKOV, L., BANKOV, N., BOCHEV, A., KUTIEV, I., TODORIEVA, L., DUBININ, E.M., PODGORNY, I.M., and POTANIN, Y.N. 1986. Suprathermal electrons in small-scale field-aligned currents. Geophysical Research Letters 13:105-108.

BEACH, R., CRESSWELL, G.R., DAVIS, T.N., HALLINAN, T.J., and SWEET, L.R. 1968. Flickering, a 10-cps fluctuation within bright auroras. Planetary and Space Science 16:1525-1529.

BENSON, R.F., and AKASOFU, S.-I. 1984. Auroral kilometric radiation/aurora correlation. Radio Science 19:527-541.

BINGHAM, R., BRYANT, D.A., and HALL, D.S. 1988. Auroral electron acceleration by lower-hybrid waves. Annales Geophysicae 6:159-168.

BOROVSKY, J.E. 1988. Production of auroral kilometric radiation by gyrophase-bunched double-layer-emitted electrons: Antennae in the magnetospheric current regions. Journal of Geophysical Research 93:5727-5740.

BOROVSKY, J.E., and JOYCE, G. 1983. Numerically simulated two-dimensional auroral double layers. Journal of Geophysical Research 88:3116-3126.

CALVERT, W. 1987. Auroral precipitation caused by auroral kilometric radiation. Journal of Geophysical Research 92:8792-8794.

CHUBB, T.A., and HICKS, G.T. 1970. Observations of the aurora in the far ultraviolet from OGO-4. Journal of Geophysical Research 75:1290-1311.

CURRIE, B.W. 1955. Auroral heights over west-central Canada. Canadian Journal of Physics 33:773-779.

DAVIS, T.N. 1966. The application of image orthicon techniques to auroral observation. Space Science Reviews 6:222-247.

———. 1978. Observed characteristics of auroral forms. Space Science Reviews 22:77-113.

EATHER, R.H. 1980. Majestic lights. Washington: American Geophysical Union.

ELVEY, C.T. 1957. Problems of auroral morphology. Proceedings of the National Academy of Sciences of the United States of America 43:63-75.

EVANS, S. 1959. Horizontal movements of visual auroral features. Journal of Atmospheric and Terrestrial Physics 16:191-193.

FINK, M., and INGRAM, J. 1972. Theoretical electron scattering amplitudes and spin polarizations. Atomic Data 4:129-207.

FRANK, L.A., CRAVEN, J.D., ACKERSON, K.L., ENGLISH, M.R., EATHER, R.H., and CAROVILLANO, R.L. 1981. Global auroral imaging instrumentation for the Dynamics Explorer mission. Space Science Instrumentation 5:369-393.

FRANK, L.A., CRAVEN, J.D., and RAIRDEN, R.L. 1985. Images of the earth's aurora and geocorona from the Dynamics Explorer mission. Advances in Space Research 5(4):53-68.

GALEEV, A.A. 1983. Anomalous resistivity on auroral field lines and its role in auroral particle acceleration. In: Hultqvist, B., and Hagfors, T., eds. High-latitude space plasma physics. New York: Plenum. 437-452.

GOERTZ, C.K. 1984. Kinetic Alfven waves on auroral field lines. Planetary and Space Science 32:1387-1392.

GOLDSTEIN, H., and SCHINDLER, K. 1978. On the role of the ionosphere in substorms: Generation of field-aligned currents. Journal of Geophysical Research 83:2574-2578.

HAERENDEL, G. 1983. An Alfven wave model of auroral arcs. In: Hultqvist, B., and Hagfors, T., eds. High-latitude space plasma physics. New York: Plenum. 515-535.

HALLINAN, T.J., and DAVIS, T.N. 1970. Small-scale auroral arc distortions. Planetary and Space Science 18:1735-1744.

HARE, F.K., and HAY, J.E. 1974. The climate of Canada and Alaska. In: Bryson, R.A., and Hare, F.K., eds. Climates of North America. New York: Elsevier. 49-192, Appendix I.

HEDIN, A.E. 1987. MSIS-86 thermospheric model. Journal of Geophysical Research 92:4649-4662.

HIRAO, K., and ITOH, T. 1978. Scientific satellite Kyokko (EXOS-A). Solar Terrestrial Environmental Research in Japan 2:148-152.

HULTQVIST, B. 1971. On the production of a magnetic-field-aligned electric field by the interaction between the hot magnetospheric plasma and the cold ionosphere. Planetary and Space Science 19:749-759.

INTERNATIONAL TELEPHONE AND TELEGRAPH CORPORATION. 1968. Reference data for radio engineers. 6th ed. New York: Sams. Section 41.

JOHNSON, R.G. 1983. The hot ion composition, energy, and pitch angle characteristics above the auroral zone ionosphere. In: Hultqvist, B., and Hagfors, T., eds. High-latitude space plasma physics. New York: Plenum. 271-294.

KIM, J.S., and VOLKMAN, R.A. 1963. Thickness of zenithal auroral arc over Fort Churchill, Canada. Journal of Geophysical Research 68:3187-3190.

KIRBY, R.C. 1982. Radio-wave propagation. In: Fink, D.G., and Christiansen, D., eds. Electronics engineers' handbook. 2nd ed. New York: McGraw-Hill. 18-50 – 18-126.

LANZEROTTI, L.J., and UBEROI, C. 1988. Earth's magnetic environment. Sky and Telescope, October:360-362.

LASSEN, K., and DANIELSEN, C. 1989. Distribution of auroral arcs during quiet geomagnetic conditions. Journal of Geophysical Research 94:2587-2594.

LENNARTSSON, W. 1977. On the role of magnetic mirroring in the auroral phenomena. Astrophysics and Space Science 51:461-495.

LOTKO, W. 1986. Diffusive acceleration of auroral primaries. Journal of Geophysical Research 91:191-203.

MAGGS, J.E., and DAVIS, T.N. 1968. Measurements of the thicknesses of auroral structures. Planetary and Space Science 16:205-209.

MARMIER, P., and SHELDON, E. 1969. Physics of nuclei and particles. Vol. I. New York: Academic.

McFADDEN, J.P., CARLSON, C.W., and BOEHM, M.H. 1990. Structure of an energetic narrow discrete arc. Journal of Geophysical Research 95:6533-6547.

MURPHREE, J.S., ELPHINSTONE, R.D., COGGER, L.L., and WALLIS, D.D. 1989. Short-term dynamics of the high-latitude auroral distribution. Journal of Geophysical Research 94:6969-6974.

OGAWA, T., and SATO, T. 1971. New mechanism of auroral arcs. Planetary and Space Science 19:1393-1412.

OGUTI, T., KITAMURA, T.-I., and WATANABE, T. 1988. Global aurora dynamics campaign, 1985-1986. Journal of Geomagnetism and Geoelectricity 40:485-504.

OLIVER, N.J., MARKHAM, T.P., and CARRIGAN, A.L. 1960. The ionosphere. In: United States Air Force Handbook of Geophysics. New York: MacMillan. 15-2 – 15-36.

OMHOLT, A. 1971. The optical aurora. New York: Springer-Verlag. Section 2.6.

ONO, T., EJIRI, M., and HIRASAWA, T. 1987. Monochromatic auroral images observed at Syowa station, in Antarctica. Journal of Geomagnetism and Geoelectricity 39:65-95.

RILEY, M.E., MacCALLUM, C.J., and BIGGS, F. 1975. Theoretical electron-atom elastic scattering cross sections. Atomic Data and Nuclear Data Tables 15:443-476.

ROGERS, E.H., NELSON, D.F., and SAVAGE, R.C. 1974. Auroral photography from a satellite. Science 183:951-952.

ROSTOKER, G., and BOSTROM, R. 1976. A mechanism for driving the gross Birkeland current configuration in the auroral oval. Journal of Geophysical Research 81:235-244.

SATO, T., and IIJIMA, T. 1979. Primary source of large-scale Birkeland currents. Space Science Reviews 24:347-366.

SAWCHUK, W., and ANGER, C.D. 1972. A dual wavelength ground-based auroral scanner. Planetary and Space Science 20:1935-1940.

STOFFREGEN, W. 1962. I.G.Y. ascaplots. Annals of the International Geophysical Year 20:1-364. Section 3.

STORMER, C. 1955. The polar aurora. London: Oxford. Chap. 8.

SWIFT, D.W. 1979. An equipotential model for auroral arcs: The theory of two-dimensional laminar electrostatic shocks. Journal of Geophysical Research 84:6427-6434.

WALLIS, D.D. 1976. Comparison of auroral electrojets and the visible aurora. In: McCormac, B.M., ed. Magnetospheric particles and fields. Dordrecht: Reidel. 247-255.